PHYSICAL REVIEW D **75,** 043011 (2007)

Evolution of polarization orientations in a flat universe with vector perturbations: CMB and quasistellar objects

Juan Antonio Morales* and Diego Sáez†

Departament d'Astronomia i Astrofísica, Universitat de València, 46100 Burjassot, València, Spain.

(Received 17 November 2006; published 26 February 2007)

Various effects produced by vector perturbations (vortical peculiar velocity fields) of a flat Friedmann-Robertson-Walker background are considered. In the presence of this type of perturbations, the polarization vector rotates. A formula giving the rotation angle is obtained and, then, it is used to prove that this angle depends on both the observation direction and the emission redshift. Hence, rotations are different for distinct quasars and also for the cosmic microwave background (CMB) radiation coming along different directions (from distinct points of the last scattering surface). As a result of these rotations, some correlations could appear in an initially random field of quasar polarization orientations. Furthermore, the polarization correlations of the CMB could undergo alterations. Quasars and CMB maps are both considered in this paper. In the case of *linear* vector modes with very large spatial scales, the maximum rotation angles appear to be of a few degrees for quasars (located at redshifts $z < 2.6$) and a few tenths of degree for the CMB. These last rotations produce contributions to the B mode of the CMB polarization which are too small to be observed with PLANCK (in the near future); however, these contributions are large enough to be observed with the next generation of satellites, which are being designed to detect the small B mode produced by primordial gravitational waves.

DOI: 10.1103/PhysRevD.75.043011 PACS numbers: 98.70.Vc, 98.54.Aj, 98.80.Es, 98.80.Jk

I. INTRODUCTION

The most general perturbation of a Friedmann-Robertson-Walker (FRW) background is the superimposition of scalar, vector, and tensor modes [1]. Scalar modes describe mass fluctuations, tensor modes are gravitational waves, and vector modes are vortical peculiar velocity fields. These last modes are not usually considered because they are not produced either during inflation or in other phase transitions produced by scalar fields in the early universe; however, there are vector perturbations in brane-world cosmologies [2] and also in models with appropriate topological defects [3]. Whatever the origin of the vector modes may be, we are interested in their possible effects. The analysis of some of these effects is our main goal.

Five decades ago, Skrotskii [4] used Maxwell equations and a perturbation of the Minkowski metric (describing a slowly rotating body) to conclude that the polarization vector rotates as the radiation crosses this space-time. This rotation (hereafter called the Skrotskii effect) is analogous to that produced by magnetic fields (Faraday effect); however, its origin is gravitational and it is wavelength independent. See Refs. [4–16] for estimates of Skrotskii rotations in several space-times. Here, these rotations are calculated in a new case: a perturbed flat FRW universe including large scale vector modes.

In the geometrical optics approximation, the polarization vector lies in the 2-plane orthogonal to the line of sight, where a basis must be chosen to define an orientation angle, ψ, for the polarization vector (that formed by this vector and another one of the chosen basis). The polarization angle ψ varies along the light trajectory because the basis is not parallely transported along the null geodesics, whereas the polarization vector parallely propagates. This idea (interpretation of the Skrotskii effect [17]) is used in Sec. II to derive an integral formula giving the total variation, $\delta\psi$, of the polarization direction, from emission to observation. Our general formula is used to prove that, in a flat FRW universe with vector perturbations, the angle $\delta\psi$ depends on both the source redshift z_e and the observation direction (unit vector $\vec{n}$). The following question arises: Which are the main effects produced by this type of rotation?

Since Skrotskii rotations change the polarization orientations and the changes are different for distinct point sources (z_e and $\vec{n}$ dependence), the statistical properties of an initial distribution (at emission time) of polarization angles is expected to be altered by the Skrotskii rotations. These statistical effects are the kind of effects we are looking for. Could we measure these effects under some conditions? Which are the most interesting cosmological sources of polarized radiation to be studied from a statistical point of view? Two types of cosmological sources are considered: the points of the last scattering surface, which can be considered as the sources of the cosmic microwave background (CMB), and the distribution of quasistellar objects (QSOs). Both cases are studied in the next sections by using appropriate simulations.

Skrotskii rotations alter the initial angular correlations (at $z_e \simeq 1100$) of the CMB polarization. In other words, they change the E and B polarization modes (see Sec. VI A). Moreover, these rotations induce correlations

*Electronic address: antonio.morales@uv.es
†Electronic address: diego.saez@uv.es

in the random initial distribution of quasar polarization orientations. This effect reminds us (1) of observations based on the analysis of radio emission from quasars (reported by Birch [18] at the early eighties), which led to the conclusion that the orientations of the quasar polarization vectors are not random, and (2) of recent polarimetric observations of hundreds of optical quasars [19], which strongly suggest that the observed polarization vectors are coherently oriented over huge regions having sizes of the order of 1 Gpc. See [20–22] for some explanation of this type of observation in the arena of *new physics*.

Birch proposed a global rotation of the Universe to explain his observations and, moreover, a rotating Bianchi type-VII_h universe has been recently proposed [23] to explain some features of the WMAP (Wilkinson Microwave Anisotropy Probe) angular power spectrum (low multipoles, asymmetry, non-Gaussian cold spots, and so on). In this paper, vector modes with appropriate scales are proposed—against a global rotation—to study both correlations in quasar polarization directions and some CMB properties. Since the evolution of nonlinear distributions of vector modes has not been described yet, we are constrained to work in the linear case.

The analysis of temperature maps of the CMB, galaxy surveys, and far supernovae lead to the so-called *concordance cosmological model*, which is a perturbation of the flat FRW background with cold dark matter and a cosmological constant. By this reason, curved backgrounds are not considered along the paper. A reduced Hubble constant $h = 10^{-2}H_0 = 0.71$ (where H_0 is the Hubble constant in units of $\mathrm{Km\,s^{-1}\,Mpc^{-1}}$), and the density parameters of vacuum energy and matter (baryonic plus dark) $\Omega_\Lambda = 0.73$ and $\Omega_m = 0.27$, respectively, are compatible with the analysis of 3 yr WMAP data recently published [24].

Along this paper, Greek (Latin) indexes run from 0 to 3 (1 to 3), and units are defined in such a way that $c = \kappa = 1$ where c is the speed of light and $\kappa = 8\pi G/c^4$ is the Einstein constant.

This article is organized as follows. In Sec. II, vector perturbations of a flat FRW background are assumed and, then, the variation, $\delta\psi$, of the polarization angle is calculated. In next section, some quantities describing the perturbed universe are expanded using *vector harmonics* and a new integral formula for $\delta\psi$ is derived in terms of the expansion coefficients. The evolution of these coefficients in the matter and radiation dominated eras is discussed in Secs. IV A and IV B, respectively. The $\delta\psi$ values corresponding to various distributions of vector modes are calculated in Secs. V and VI. In Sec. V, only a vector mode is considered and angles $\delta\psi$ are calculated for different spatial scales of this mode and also for distinct emission redshifts. Taking into account results of Sec. V, two appropriate superimpositions of vector modes are studied in Sec. VI. In Secs. VI A and VI B the chosen superimpositions are linear in the redshift intervals (0,1100) and (0,2.6), respectively. In the first (second) case, angles $\delta\psi$ are calculated for the CMB (quasars at $z < 2.6$). Finally, Sec. VII is a general discussion of the main results obtained in the paper and also a summary of conclusions and perspectives.

II. POLARIZATION ANGLE: DEFINITION AND EVOLUTION

In practice, calculations in a perturbed FRW universe require the use of a certain gauge (see Ref. [1] for definition and examples). Whatever the gauge may be, the line element of the flat FRW background and that of the perturbed (real) universe can be written in the form:

$$ds^2 = a^2(\eta)\eta_{\mu\nu}dx^\mu dx^\nu = a^2(\eta)[-d\eta^2 + dr^2 + r^2(d\theta^2 + \sin^2\theta d\phi^2)] \quad (1)$$

and

$$ds^2 = g_{\mu\nu}dx^\mu dx^\nu = a^2(\eta)(\eta_{\mu\nu} + h_{\mu\nu})dx^\mu dx^\nu, \quad (2)$$

respectively, where a is the scale factor (whose present value is assumed to be $a_0 = 1$), η is the conformal time, $\eta_{\mu\nu}$ is the Minkowski metric, and the small first order quantities $h_{\mu\nu}$ define the perturbation. Admissible restrictions satisfied by some of the $h_{\mu\nu}$ quantities can be used to fix the gauge. As it is well known, scalar, vector, and tensor linear modes undergo independent evolutions and, consequently, only vector modes are hereafter considered. In this situation, the condition $h_{ij} = 0$ defines the gauge used in all our calculations, and the absence of scalar perturbations implies the relation $h_{00} = 0$.

Hereafter, $\{r, \theta, \phi\}$ are spherical coordinates associated to x^i and $\{e_r, e_\theta, e_\phi\}$ are unit vectors parallel to the coordinate ones. The chosen gauge allows us to define the polarization angle ψ in the most operating way. It is due to the fact that vectors $\{e_r, e_\theta, e_\phi\}$ are orthogonal among them ($h_{ij} = 0$) and, consequently, observers receiving radiation in the direction e_r can use vectors e_θ and e_ϕ as a basis in the plane orthogonal to the propagation direction (where the polarization vector $\vec{P}$ lies). In this basis, the polarization vector can be written in the form

$$\vec{P} = P(\cos\psi e_\theta + \sin\psi e_\phi), \quad (3)$$

and, then, the polarization angle is that formed by $\vec{P}$ and e_θ.

Using the notation $h_{0i} = (h_1, h_2, h_3) \equiv \vec{h}$, the line element of Eq. (2) can be written as follows:

$$ds^2 = a^2(-d\eta^2 + 2h_i dx^i d\eta + \delta_{ij}dx^i dx^j). \quad (4)$$

An orthonormal tetrad for the corresponding metric is given by

$$e_0 = \frac{1}{a}\left(\frac{\partial}{\partial\eta} - h^i\frac{\partial}{\partial x^i}\right), \qquad e_r = \frac{1}{a}\frac{\partial}{\partial r},$$
$$e_\theta = \frac{1}{ar}\frac{\partial}{\partial\theta}, \qquad e_\phi = \frac{1}{ar\sin\theta}\frac{\partial}{\partial\phi}, \tag{5}$$

where $h^i = \delta^{ij}h_j$.

The parallel propagation of the polarization vector along null geodesics leads to

$$\nabla_l\vec{P} = 0, \tag{6}$$

where ∇_l stands for the covariant derivative along the geodesic null vector l associated with radiation propagation and, as a consequence, the magnitude of $\vec{P}$ is constant along each null geodesic ($\nabla_l P = 0$). Substitution of Eq. (3) into Eq. (6) leads to

$$\nabla_l\psi = -g(e_\phi, \nabla_l e_\theta) = g(e_\theta, \nabla_l e_\phi). \tag{7}$$

Note that the second equality directly follows from the orthogonality of e_θ and e_ϕ, that is $g(e_\theta, e_\phi) = 0$. In the considered coordinate frame one has $l = l^\mu\partial_\mu$ and

$$\nabla_l e_\theta = \nabla_l\left(\frac{1}{ar}\frac{\partial}{\partial\theta}\right) = l^\mu\left[\partial_\mu\left(\frac{1}{ar}\right)\frac{\partial}{\partial\theta} + \frac{1}{ar}\Gamma^\nu_{\mu\theta}\frac{\partial}{\partial x^\nu}\right]. \tag{8}$$

Since we are using the orthonormal tetrad of Eq. (5), the variation of the polarization angle along l is

$$\nabla_l\psi = -\frac{1}{a^2r^2\sin\theta}l^\mu\Gamma_{\mu\theta.\phi}. \tag{9}$$

By substituting the Christoffel symbols $\Gamma_{\mu\theta.\phi} = \Gamma^\nu_{\mu\theta}g_{\nu\phi}$ of the metric (4) into Eq. (9) one obtains

$$\frac{d\psi}{d\lambda} = -\frac{1}{2r^2\sin\theta}\left(\frac{\partial h_{\eta\phi}}{\partial\theta} - \frac{\partial h_{\eta\theta}}{\partial\phi}\right)\frac{d\eta}{d\lambda} - \cos\theta\frac{d\phi}{d\lambda}, \tag{10}$$

where λ is the affine parameter of the null geodesic whose tangent vector is $l^\mu = \frac{dx^\mu}{d\lambda}$. Equation (10) holds for nonlinear modes; however, vector perturbations are hereafter assumed to be linear. The reason of this restrictive condition is that no evolution equations are known for nonlinear vector modes. We are studying this case, but it seems to be a rather complicated problem whose study is out of the scope of this basic work.

In order to obtain the overall change, $\delta\psi$, of the polarization angle, an integration based on Eq. (10) must be performed from observation to emission points. Up to first order, this integration can be done along the associated radial null geodesic of the flat FRW background, which satisfies the equations $\dot{\eta} = -\dot{r}$, $\dot{\theta} = \dot{\phi} = 0$, where the dot stands for the derivative with respect to an affine parameter; hence, from Eq. (10), the total variation of ψ appears to be

$$\delta\psi = \frac{1}{2\sin\theta}\int_{r_e}^{0}\left(\frac{\partial h_{\eta\phi}}{\partial\theta} - \frac{\partial h_{\eta\theta}}{\partial\phi}\right)\frac{dr}{r^2}, \tag{11}$$

where r_e is the radial coordinate at emission.

Let us now use Cartesian coordinates $x = r\sin\theta\cos\phi$, $y = r\sin\theta\sin\phi$, $z = r\cos\theta$ in the flat background metric (1). In these coordinates one easily gets

$$\frac{\partial h_{\eta\phi}}{\partial\theta} - \frac{\partial h_{\eta\theta}}{\partial\phi} = r^2\sin\theta A^{ij}\frac{\partial h_{0i}}{\partial x^j}, \tag{12}$$

where the nonzero elements of the skew-symmetric matrix A^{ij} are

$$A^{12} = -\cos\theta, \qquad A^{13} = \sin\theta\sin\phi,$$
$$A^{23} = -\sin\theta\cos\phi. \tag{13}$$

After performing this last coordinate transformation, Eq. (11) can be rewritten as follows:

$$\delta\psi = -\frac{1}{2}\int_0^{r_e}(\vec{\nabla}\times\vec{h})\cdot\vec{n}dr, \tag{14}$$

where $\vec{n} = \vec{r}/r = (\sin\theta\cos\phi, \sin\theta\sin\phi, \cos\theta)$ is the unit vector in the chosen radial direction (constant θ and ϕ coordinates). Equation (14) gives what is hereafter called the Skrotskii cosmological effect (or rotation). Note that $\vec{\nabla}$ and the dot stand for the covariant derivative and the scalar product with respect to the background flat three-dimensional metric, respectively; hence, the Skrotskii rotation is obtained by integrating the curl of the vector perturbation $\vec{h}$ along the line of sight. In the absence of vector modes ($\vec{h} = 0$) one finds $\delta\psi = 0$, which means that there are no Skrotskii rotations in a flat FRW universe. The same can be proved easily for curved unperturbed FRW universes and also for flat and curved universes including pure linear scalar modes.

III. SKROTSKII ROTATIONS PRODUCED BY VECTOR MODES

In this section, we use the formalism described in Refs. [1,25], in which the cosmological vector perturbations are developed in terms of appropriate functions. In the case of a flat FRW background, these functions are combinations of plane waves and, consequently, the mentioned modes are defined in Fourier space.

Vector modes contribute to the metric perturbation $\vec{h}$, which is written in the form

$$\vec{h}(\eta, \vec{r}) = -\int\vec{f}(\eta, \vec{r}, \vec{k})d^3k, \tag{15}$$

where vector $\vec{f}$ is the following linear combination:

$$\vec{f}(\eta, \vec{r}, \vec{k}) = B^+(\eta, \vec{k})\vec{Q}^+(\vec{r}, \vec{k}) + B^-(\eta, \vec{k})\vec{Q}^-(\vec{r}, \vec{k}) \tag{16}$$

of the modes $\vec{Q}^\pm$. This combination is hereafter denoted in a more compact form:

$$\vec{f}(\eta, \vec{r}, \vec{k}) = B^{\pm}(\eta, \vec{k})\vec{Q}^{\pm}(\vec{r}, \vec{k}). \quad (17)$$

Since $\vec{h}$ is a real vector, coefficients $B^{\pm}$ must satisfy the condition

$$B^{\pm}(\eta, \vec{k}) = -(B^{\pm})^{*}(\eta, -\vec{k}), \quad (18)$$

where the star stands for complex conjugation. For each k mode, $\vec{Q}^{\pm}$ are fundamental harmonic vectors, that is, divergence-free eigenvectors of the Laplace operator Δ corresponding to the flat three-dimensional Euclidean metric ($\vec{\nabla}\cdot\vec{Q}^{\pm} = 0$ and $\Delta\vec{Q}^{\pm} = -k^2\vec{Q}^{\pm}$ with $k = \sqrt{\vec{k}\cdot\vec{k}}$). By choosing the representation used in Ref. [25], the $\vec{Q}^{\pm}$'s are written in the form

$$\vec{Q}^{\pm}(\vec{r}, \vec{k}) = \vec{\epsilon}^{\pm}(\vec{\kappa})\exp(i\vec{k}\cdot\vec{r}), \quad (19)$$

where $\vec{\epsilon}^{\pm}(\vec{\kappa}) = -\frac{i}{\sqrt{2}}(\vec{e}_1 \pm i\vec{e}_2)$ and vectors $\{\vec{e}_1, \vec{e}_2, \vec{\kappa}\}$ form a positively oriented orthonormal basis, $\vec{e}_1 \times \vec{e}_2 = \vec{\kappa} \equiv \vec{k}/k$. In a standard orthonormal basis in which $\vec{k} = (k_1, k_2, k_3)$, we can choose

$$\vec{e}_1 = (k_2, -k_1, 0)/\sigma_1, \qquad \vec{e}_2 = (k_1k_3, k_2k_3, -\sigma_1^2)/\sigma_2, \quad (20)$$

with the obvious notation

$$\sigma_1 = \sqrt{k_1^2 + k_2^2}, \qquad \sigma_2 = k\sigma_1.$$

In such a basis, which is used to perform numerical estimations in next sections, one can write $\vec{\epsilon}^{\pm} = (\epsilon_1^{\pm}, \epsilon_2^{\pm}, \epsilon_3^{\pm})$ with

$$\epsilon_1^{\pm} = \frac{1}{\sqrt{2}}\left(\pm\frac{k_1k_3}{\sigma_2} - i\frac{k_2}{\sigma_1}\right), \quad (21)$$

$$\epsilon_2^{\pm} = \frac{1}{\sqrt{2}}\left(\pm\frac{k_2k_3}{\sigma_2} + i\frac{k_1}{\sigma_1}\right), \quad (22)$$

$$\epsilon_3^{\pm} = \mp\frac{1}{\sqrt{2}}\frac{\sigma_1^2}{\sigma_2}. \quad (23)$$

In this representation, the following relations can be obtained easily, from Eq. (16), for each k mode:

$$\vec{\nabla}\vec{f} = iB^{\pm}\vec{k}\otimes\vec{\epsilon}^{\pm}\exp(i\vec{k}\cdot\vec{r}), \quad (24)$$

$$\vec{\nabla}\times\vec{f} = iB^{\pm}\vec{k}\times\vec{\epsilon}^{\pm}\exp(i\vec{k}\cdot\vec{r}) = k(B^{+}\vec{\epsilon}^{+} - B^{-}\vec{\epsilon}^{-})\exp(i\vec{k}\cdot\vec{r}), \quad (25)$$

where symbol $\otimes$ ($\times$) stands for the tensor (vector) product. We have taken into account the relation $\vec{\epsilon}^{\pm}\times\vec{\kappa} = \pm i\vec{\epsilon}^{\pm}$ to obtain the second equality in Eq. (25). From Eqs. (14) and (25), the contribution of each k mode to the rotation of the polarization angle ψ is found to be $\delta\psi_k = \delta\psi_k^{+} + \delta\psi_k^{-}$, where

$$\delta\psi_k^{+} = \frac{k}{2}\vec{n}\cdot\vec{\epsilon}^{+}(\vec{\kappa})\int_0^{r_e} B^{+}(\eta, \vec{k})\exp(i\vec{k}\cdot\vec{r})dr \quad (26)$$

and

$$\delta\psi_k^{-} = -\frac{k}{2}\vec{n}\cdot\vec{\epsilon}^{-}(\vec{\kappa})\int_0^{r_e} B^{-}(\eta, \vec{k})\exp(i\vec{k}\cdot\vec{r})dr. \quad (27)$$

The integrals can be performed along a radial null geodesic of the FRW background. Note that the explicit $\vec{\kappa}$ dependence of $\vec{\epsilon}^{\pm}$, that is function $\vec{\epsilon}^{\pm}(\vec{\kappa})$, is given by Eqs. (21)–(23). Finally, the total Skrotskii cosmological rotation produced by a distribution of vector modes (vortical field of peculiar velocities) is $\delta\psi = \delta\psi^{+} + \delta\psi^{-}$, where

$$\delta\psi^{\pm} = \int \delta\psi_k^{\pm} d^3k. \quad (28)$$

IV. EINSTEIN EQUATIONS FOR VECTOR PERTURBATIONS

According to Eqs. (26)–(28), the total Skrotskii effect depends on the coefficients (functions) $B^{\pm}(\eta, \vec{k})$ appearing in the expansion of h_{0i}. These coefficients evolve coupled to other ones, which are involved in the expansions of other physical quantities. Two of these coefficients, $v^{\pm}(\eta, \vec{k})$, are related with the expansion coefficients of the matter four-velocity, $u = u^0\partial_0 + u^i\partial_i = (u^0, \vec{u})$. In terms of these two new functions, the peculiar velocity $\vec{v} = \vec{u}/u^0$ can be written as follows:

$$\vec{v}(\eta, \vec{r}, \vec{k}) = \int v^{\pm}(\eta, \vec{k})\vec{Q}^{\pm}(\vec{r}, \vec{k})d^3k; \quad (29)$$

moreover, there are two coefficients, $\Pi^{\pm}(\eta, \vec{k})$, which appear in the expansion of E_{ij}/p_b, where p_b is the background pressure and E_{ij} the traceless tensor describing anisotropic stresses (see [1]).

The expansions of $\vec{h}$, $\vec{v}$, and E_{ij}/p_b must be introduced into Einstein equations to get evolution and constraint equations for the coefficients $B^{\pm}$, $v^{\pm}$, and $\Pi^{\pm}$. After solving these equations we can use the resulting function $B^{\pm}(\eta, \vec{k})$ to perform the integrals in Eqs. (26) and (27). In the chosen gauge, if the background is flat and there are no scalar and tensor modes, Einstein equations lead to the following evolution equation for $B^{\pm}$:

$$\frac{k}{2}\frac{d}{d\eta}(B^{\pm}a^2) = -a^4p_b\Pi^{\pm}(\eta), \quad (30)$$

and also to the constraint

$$\frac{1}{2}\frac{k^2}{a^2}B^{\pm} = (\rho_b + p_b)v_c^{\pm}, \quad (31)$$

where ρ_b (p_b) stands for the background density (pressure), and

$$v_c^{\pm} = v^{\pm} - B^{\pm} \quad (32)$$

is a gauge invariant quantity (see [1]) that measures the

amplitude of the matter vorticity. Since we are considering the concordance model, there are a cosmological constant and, consequently, we can write the equations $\rho_b = \rho_\Lambda + \rho_b^{rm}$ and $p_b = p_\Lambda + p_b^{rm}$, where ρ_Λ and p_Λ (ρ_b^{rm} and p_b^{rm}) are the energy density and pressure of the vacuum (radiation plus matter in the background), respectively. Equation $\rho_\Lambda + p_\Lambda = 0$ is always satisfied. In the radiation dominated era, one can write $\rho_b \simeq \rho_b^r$ and $p_b \simeq p_b^r = w\rho_b^r$, where ρ_b^r and p_b^r are the radiation energy density and pressure in the background, respectively. Parameter w takes on the value $\frac{1}{3}$ and the sound speed in the background is $c_s = \frac{1}{\sqrt{3}}$. Finally in the matter dominated era one has $\rho_b \simeq \rho_\Lambda + \rho_b^m$ and $p_b \simeq p_\Lambda$, where ρ_b^m is the background energy density of matter. Since the background pressure of matter p_b^m is negligible in this era, we write $w = c_s = 0$, in other words, we assume that, during the matter dominated era, quantities w and c_s are those associated to the matter fluid (not to the vacuum). Taking into account these assumptions relative to w and c_s, simple manipulations of Eqs. (30) and (31) lead to the following equations, which are valid during any era:

$$\dot{v}_c^{\pm} = \frac{\dot{a}}{a}(3c_s^2 - 1)v_c^{\pm} - k\frac{p_b}{\rho_b^{mr} + p_b^{mr}}\Pi^{\pm}(\eta), \tag{33}$$

and

$$B^{\pm} = 2\frac{a^2}{k^2}(\rho_b^{mr} + p_b^{mr})v_c^{\pm}. \tag{34}$$

Equation (33) can be also directly obtained from the (contracted) Bianchi identities. This equation is used to calculate $v_c^{\pm}(\eta, \vec{k})$; afterward, Eq. (34) gives the function $B^{\pm}(\eta, \vec{k})$, which is necessary to estimate the Skrotskii effect and, finally, Eq. (32) allows us to calculate the coefficient $v^{\pm}$ associated with the peculiar velocity in the gauge under consideration. Now, let us study Eqs. (33) and (34) in the different cosmological eras.

A. Matter dominated era

From emission to observation, the radiation emitted by any quasar as well as the CMB radiation coming from the last scattering surface evolve in the matter dominated era, at redshift $z < 1100$; namely, before and during vacuum energy domination. In this phase, taking into account previous comments given in this section and the relation $\rho_b^m \propto a^{-3}$, Eq. (33) can be written easily as follows:

$$\dot{v}_c^{\pm} = -\frac{\dot{a}}{a}v_c^{\pm} + k\frac{\Omega_\Lambda}{\Omega_m}a^3\Pi^{\pm}. \tag{35}$$

In the absence of anisotropic stresses ($\Pi^{\pm} = 0$), the solution of the last equation is

$$v_c^{\pm} = \frac{v_{c0}^{\pm}}{a}. \tag{36}$$

From Eqs. (34) and (36) the following relation is easily derived:

$$B^{\pm}(\eta, \vec{k}) = \frac{6H_0^2\Omega_m v_{c0}^{\pm}(\vec{k})}{k^2a^2(\eta)}, \tag{37}$$

and, then, from Eqs. (26)–(28) and (37), the total Skrotskii effect is found to be

$$\delta\psi = 3H_0^2\Omega_m\int_0^{r_e}\frac{dr}{a^2(r)}[\vec{n}\cdot\vec{F}(\vec{r})], \tag{38}$$

where

$$\vec{F}(\vec{r}) = \int\frac{v_{c0}^{+}\vec{\epsilon}^{+}(\vec{\kappa}) - v_{c0}^{-}\vec{\epsilon}^{-}(\vec{\kappa})}{k}\exp(i\vec{k}\cdot\vec{r})d^3k. \tag{39}$$

Function $a = a(r)$ is implicitly defined by the relation (44) and it is numerically computed before any numerical calculation of the integrals in Eqs. (38) and (39). Finally, Eqs. (15), (16), and (37) lead to a metric perturbation of the form

$$\vec{h}(\eta, \vec{r}) = -6H_0^2\Omega_m a^{-2}(\eta)\int\frac{v_{c0}^{\pm}(\vec{k})}{k^2}\vec{\epsilon}^{\pm}(\vec{\kappa})\exp(i\vec{k}\cdot\vec{r})d^3k, \tag{40}$$

where $v_{c0}(\vec{k}) = -v_{c0}^{*}(-\vec{k})$ to ensure that Eq. (18) is satisfied. Finally, the gauge invariant velocity is

$$\vec{v}_c^{\pm}(\eta, \vec{r}) = a^{-1}(\eta)\int v_{c0}^{\pm}(\vec{k})\vec{\epsilon}^{\pm}(\vec{\kappa})\exp(i\vec{k}\cdot\vec{r})d^3k. \tag{41}$$

The notation defined in Sec. III [see Eqs. (16) and (17)] has been used in Eqs. (29), (40), and (41). Equations. (36)–(41) are basic for the calculations in this paper.

B. Radiation dominated era

If vector modes appeared in the early universe—during some unknown phase transition—they evolved all along the radiation dominated era and, afterward, in the matter dominated era, until the period of interest ($z < 1100$). How did vector perturbations evolve during radiation domination? In that phase, Eq. (33) reduces to

$$\frac{dv_c^{\pm}}{d\eta} = -\frac{k}{4}\Pi^{\pm}(\eta), \tag{42}$$

and, Eq. (34) reads as follows:

$$B^{\pm} = \frac{8}{3}\rho_b^{r0}k^{-2}a^{-2}v_c^{\pm}, \tag{43}$$

where $\rho_b^{r0} \simeq 8\times10^{-34}$ gr/cm^3 is the present radiation energy density (CMB at $T \simeq 2.73K$). It is worthwhile to notice that the relation $\rho_b^r = \rho_b^{r0}a^{-4}$, which has been assumed in order to derive Eq. (43), is only an approximated relation which is good enough for us, nevertheless, the true law is $\rho_b^r \propto (g^*)^{4/3}a^{-4}$, where g^* gives the effective degrees of freedom due to relativistic species coupled to the CMB (see [26]). This number undergoes some variations,

which are particularly important at very high temperatures in the early radiation dominated era.

Let us first consider vanishing $\Pi^{\pm}$ coefficients. Under this assumption, the solution of Eq. (42) is $v_c^{\pm} =$ constant and, then, Eq. (43) leads to the relation $B^{\pm} \propto a^{-2}$; therefore, the coefficients $B^{\pm}(\eta, \vec{k})$ appearing in Eqs. (26) and (27) decrease as a^{-2} in both the radiation and the matter [see Eq. (37)] dominated eras. As a result of this continuous decreasing, if small vector perturbation of the background metric (vector $\vec{h}$) appeared at very high redshift (early universe), they should be negligible at redshifts $z <$ 1100 [no significant Skrotskii rotations according to Eqs. (26) and (27)].

In a universe containing a fluid with baryons, cold dark matter, and vacuum energy, there are no great enough anisotropic stresses ($\Pi^{\pm} \neq 0$) modifying the evolution of the vector modes according to Eqs. (35) and (42). In order to have nonvanishing $\Pi^{\pm}$ coefficients, some physical field having an energy momentum tensor $T_{\alpha\beta}$ with an appropriate vector contribution to T_{ij} seems to be necessary. This contribution to T_{ij} is to be expanded in vector modes [1], and it would play the same role as the anisotropic stresses of a fluid. It seems that, in order to maintain a vortical velocity field in the Universe, nonstandard fields (new physics) are necessary. In the absence of these fields ($\Pi^{\pm} = 0$), divergenceless velocities decay. In other words, either vortices are maintained ($\Pi^{\pm} \neq 0$) in some way or they must decay as a result of expansion.

Let us imagine (toy model) some field justifying the condition $\Pi^{\pm}(\eta, \vec{k}) < 0$. In such a case, Eq. (42) leads to growing $v_c^{\pm}$ functions ($dv_c^{\pm}/d\eta > 0$). The time evolution of $v_c^{\pm}$ depends on the explicit form of functions $\Pi^{\pm}(\eta, \vec{k})$. For appropriate choices of $\Pi^{\pm}(\eta, \vec{k})$ the coefficient $v_c^{\pm}$ could become proportional to any power a^n and, then, from Eq. (43) one easily get the relation $B^{\pm} \propto a^{n-2}$; hence, functions $B^{\pm}$ would be independent on time (growing functions) during the radiation dominated era for $n = 2$ ($n > 2$); afterward, in the matter dominated era, coefficients $B^{\pm}$ obey Eq. (35) and, consequently, if the sign of $\Pi^{\pm}(\eta, \vec{k})$ keeps negative, these coefficients decrease. If functions $B^{\pm}$ increase (for appropriate negative $\Pi^{\pm}$ values) during the radiation dominated era, the linear approximation could break before arriving to matter domination and, then, a fully nonlinear treatment of the problem would be necessary; moreover, quantities $B^{\pm}$ would only decay in the matter dominated era and their values at redshifts close to 1100 could be large enough to produce significant Skrotskii rotations. However, at quasar redshifts, coefficients $B^{\pm}$ would be much smaller than those corresponding to $z \simeq 1100$ and Skrotskii rotations would be negligible.

An alternative idea is that vector perturbations did not appear in the early universe, but at much more recent cosmological times; it is possible in some scenarios, for example, it is well known that bulk effects in Randall-Sundrum-type brane-world cosmologies generate vector perturbations [2] whose Skrotskii rotations will be studied elsewhere.

Hereafter, it is assumed the presence of large scale linear vector perturbations at low redshifts (without any justification for them) and, then, the associated Skrotskii rotations are estimated in the worst case, namely, when these modes are freely decaying ($\Pi^{\pm} = 0$).

Let us now use Eqs. (38) and (39) to estimate Skrotskii rotations for sources located at different redshifts and observed in distinct directions (CMB and QSOs). Calculations are performed in a universe containing appropriate distributions of vector modes.

V. SKROTSKII ROTATIONS PRODUCED BY A UNIQUE VECTOR MODE

We begin with some considerations about the spatial scales, L, of our vector modes. The analysis of the 3 yr WMAP data [27] strongly suggests that some of the $\ell < 10$ CMB multipoles are too small, which is particularly important for $\ell = 2$ (see Fig. 19 in [27]). On account of these facts, vector modes with very large spatial scales are tried in our calculations. The scales must be large enough to alter only the first multipoles of the CMB angular power spectrum. In the concordance model described in the introduction, the angle $\Delta\theta$ subtended by a comoving scale L located at the last scattering surface (at redshift $z \simeq 1/a \simeq$ 1100) is $\Delta\theta = L/\tilde{r}$, where $\tilde{r} = 14083$ Mpc is the r value given by the relation

$$r = H_0^{-1} \int_a^1 [(1 - \Omega_\Lambda)\xi + \Omega_\Lambda \xi^4]^{-1/2} d\xi \qquad (44)$$

for $a \simeq 1/1100$. Finally, taking into account the relation $\Delta\theta = \pi/\ell$, one easily concludes that the contributions to the $\ell = 5$ multipole are mainly produced by spatial scales close to $L \sim 9000$ Mpc. This means that scales larger than $L_{\min} \sim 10\,000$ Mpc could affect only small ℓ multipoles. After these considerations, we assume that the vector perturbations to be included in our model have very large spatial scales greater than 10^4 Mpc.

In order to estimate the Skrotskii rotation $\delta\psi$ produced by a unique vector mode $\vec{k}_0$, we take into account Eqs. (18) and (34) to write

$$v_{c0}^{\pm}(\vec{k}) = v_{c0}^{\pm}\delta(\vec{k} - \vec{k}_0) - (v_{c0}^{\pm})^* \delta(\vec{k} + \vec{k}_0), \qquad (45)$$

where the complex numbers $v_{c0}^{\pm} = v_{c0R}^{\pm} + i v_{c0I}^{\pm}$ fix the amplitude of the chosen mode and $\delta(\vec{k} - \vec{k}_0)$ and $\delta(\vec{k} + \vec{k}_0)$ are Dirac-distributions. After substituting the distributions $v_{c0}^{\pm}(\vec{k})$ given by Eq. (45) into Eq. (39), the integration in d^3k can be performed easily and, then, Eqs. (38) and (39) lead to the following relation:

$$\delta\psi = \frac{3H_0^2\Omega_m}{k_0}\vec{n}\cdot[v_{c0}^{+}\vec{\epsilon}^{+}(\vec{\kappa}_0) - v_{c0}^{-}\vec{\epsilon}^{-}(\vec{\kappa}_0)] \times \int_0^{r_e}\frac{\exp(i\vec{k}_0\cdot\vec{r})}{a^2(r)}dr; \quad (46)$$

moreover, vectors $\vec{v}_{c0}(\vec{r})$ and $\vec{h}_0(\vec{r})$ reduce to

$$\vec{v}_{c0}(\vec{r}) = v_{c0}^{\pm}\vec{\epsilon}^{\pm}(\vec{\kappa}_0)\exp(i\vec{k}_0\cdot\vec{r}), \quad (47)$$

and

$$\vec{h}_0(\vec{r}) = \frac{-6H_0^2\Omega_m}{k_0^2}\vec{v}_{c0}(\vec{r}). \quad (48)$$

Let us now discuss amplitudes. According to Eq. (47), the amplitude A_{v0} of the function $\vec{v}_{c0}(\vec{r})$ is fixed by numbers $v_{c0}^{\pm}$. Hence, from Eq. (48) one easily concludes that the amplitude A_{h0} of function $\vec{h}_0(\vec{r})$ is

$$A_{h0} \simeq 2\times 10^{-9}L_0^2A_{v0}, \quad (49)$$

where $L_0 = 2\pi/k_0$ must be written in megaparsecs. Moreover, from Eq. (37) it follows that the amplitude A_h at redshift z is

$$A_h = A_{h0}(1+z)^2. \quad (50)$$

It is hereafter assumed that, at any redshift, a distribution of vector modes is linear if the condition $A_h \leq 0.2$ is satisfied; hence, from Eqs. (49) and (50) one easily concludes that linearity at redshift z [which implies linearity in all the interval $(0, z)$] requires small enough A_{v0} values satisfying the relation $A_{v0} \lesssim 10^8L_0^{-2}(1+z)^{-2}$. According to this inequality, for $L_0 = 5\times 10^4$ Mpc, vector modes are linear at redshifts $z = 0$, $z = 2.6$, and $z = 1100$, if the relations $A_{v0} \leq 4\times 10^{-2}$, $A_{v0} \leq 3\times 10^{-3}$, and $A_{v0} \leq 3.3\times 10^{-8}$, respectively, are satisfied. In order to estimate Skrotskii rotations for QSOs and the CMB, linearity is assumed in the intervals (0,2.6) and (0,1100), respectively. The interval (0,2.6) is appropriate because there is a numerous sample of polarized QSOs having redshifts smaller than 2.6. On account of Eq. (47) and the definitions of vectors $\vec{\epsilon}^{\pm}(\vec{\kappa}_0)$, it is obvious that the condition $A_{v0} \leq 3\times 10^{-3}$ ($A_{v0} \leq 3.3\times 10^{-8}$) is approximately satisfied for $|v_{c0}^{\pm}| \leq 3\times 10^{-3}$ ($|v_{c0}^{\pm}| \leq 3.3\times 10^{-8}$) and, consequently, the required linearity of the vector modes is hereafter fixed by assuming $v_{c0}^{\pm}$ values satisfying these inequalities.

The angles $\delta\psi^{\pm}$ given by Eq. (46) are proportional to quantities $v_{c0}^{\pm}$, which are conditioned by our assumptions about linearity; hence, in the case of *linear* vector modes with $L_0 = 5\times 10^4$ Mpc, the greatest Skrotskii rotations are obtained for $|v_{c0}^{\pm}| = 3\times 10^{-3}$ (QSOs) and $|v_{c0}^{\pm}| = 3.3\times 10^{-8}$ (CMB). If we give more power to the scale L_0, namely, if greater values of $|v_{c0}^{\pm}|$ are assumed for this scale, it could produce greater rotations, but it would evolve beyond the linear regime (A_h values greater than 0.2). Furthermore, if the above values of $|v_{c0}^{\pm}|$ are assigned to scales $L_0 > 5\times 10^4$ Mpc, Eqs. (49) and (50) lead to the conclusion that the resulting vector modes also evolve in the nonlinear regime with $A_h > 0.2$, at least for redshifts close to $z = 2.6$ (QSOs) and $z = 1100$ (CMB). The treatment of these moderately nonlinear cases is being studied. Greater Skrotskii rotations are expected to be produced by these modes.

Finally, let us study the angular and redshift dependence of $\delta\psi$. Since only one linear mode is considered, the vector basis in the momentum space can be chosen in such a way that the components of vectors $\vec{k}_0$ and $\vec{n}$ are $(k_0, 0, 0)$ and $(\sin\theta\cos\phi, \sin\theta\sin\phi, \cos\theta)$, respectively; thus, Eqs. (21)–(23) lead to a simple representation of vectors $\vec{\epsilon}^{\pm}(\vec{\kappa}_0)$. Using this representation, Eq. (46) can be rewritten as follows:

$$\delta\psi^{\pm} = C[(I_s v_{c0I}^{\pm} - I_c v_{c0R}^{\pm})\cos\theta - (I_s v_{c0R}^{\pm} + I_c v_{c0I}^{\pm})\sin\theta\sin\phi], \quad (51)$$

where $C = 6H_0^2\Omega_m/k_0\sqrt{2}$,

$$I_s = \int_0^{r_e} a^{-2}(r)\sin\xi dr, \quad (52)$$

$$I_c = \int_0^{r_e} a^{-2}(r)\cos\xi dr, \quad (53)$$

and $\xi = rk_0\sin\theta\cos\phi$. Equation (51) has been first used to estimate the $\delta\psi^{\pm}$ angles for $v_{c0R}^{\pm} = v_{c0I}^{\pm} = 3\times 10^{-3}$. In this case one easily finds the relation $\delta\psi = \delta\psi^{+} + \delta\psi^{-} = 2[(\delta\beta - \delta\alpha)\cos\theta + (\delta\beta + \delta\alpha)\sin\theta\sin\phi]$, where $\delta\alpha = 0.003CI_c$ and $\delta\beta = 0.003CI_s$ ($\delta\alpha$ and $\delta\beta$ are the angles represented in Fig. 1). In order to estimate the values of $\delta\psi$, quantities $\delta\alpha$ and $\delta\beta$ have been always calculated for $\theta = \pi/4$ and $\phi = \pi/2$. First, a fixed quasar redshift $z = 2.6$ (comoving distance of ~6000 Mpc) and variable k_0 values have been considered. Results are presented in the top panel of Fig. 1, where it is seen that the resulting $\delta\alpha$ (solid line) and $\delta\beta$ (dotted line) values are not negligible only for large spatial scales greater than $\sim 10^4$ Mpc, which are the scales we are interested in (see above). Moreover, quantities $\delta\alpha$ and $\delta\beta$ have been calculated for a fixed spatial scale of 5×10^4 Mpc and for variable redshifts (quasar positions); the central panel of Fig. 1 shows the results. Both quantities grow as the redshift increases, reaching values of a few degrees for large enough redshifts. Finally, in the bottom panel of Fig. 1, quantities $\delta\alpha$ and $\delta\beta$ correspond to $z = 1100$ (CMB) and $v_{c0R}^{\pm} = v_{c0I}^{\pm} = 3.3\times 10^{-8}$ [linear vector perturbation in the interval (0,1100)]. In this last panel, the $\delta\alpha$ and $\delta\beta$ angles reach values of a few tenths of degree for large L_0 values close to 5×10^4 Mpc.

Equations (51)–(53) indicate that the rotation angles depend on the observation direction. Apart from the explicit dependence on θ and ϕ displayed in Eq. (51), there is a smoother dependence due to the fact that quantities I_c and I_s depend on the bounded functions $\cos\xi$ and $\sin\xi$ [see Eqs. (52) and (53)]. In general, the angle $\delta\psi$ is a combi-

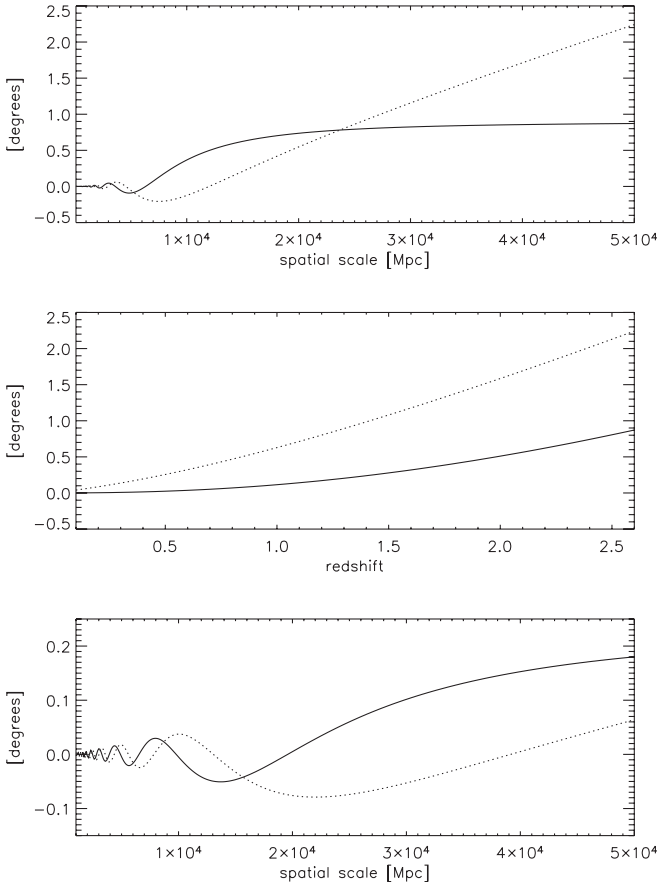

FIG. 1. Top: dotted (solid) line gives the angle $\delta\alpha$ ($\delta\beta$) in terms of the spatial scale, in megaparsecs, for $z = 2.6$. Central: dotted (solid) line gives the angle $\delta\alpha$ ($\delta\beta$) as a function of z for a spatial scale of 5×10^4 Mpc. Bottom: the same as in the top panel for $z = 1100$ (CMB). In all cases, vector modes have been forced to be linear.

nation of the quantities $\delta\alpha$ and $\delta\beta$ exhibited in Fig. 1 whose coefficients depend on angles θ and ϕ [see Eq. (51)]. This general dependence has been restricted because the four quantities $v^{\pm}_{c0R}$ and $v^{\pm}_{c0I}$ have been assumed to be identical (approximating condition allowing a good enough estimate of Skrotskii rotations).

VI. SUPERIMPOSING VECTOR MODES. SIMULATIONS

In Sec. V, the rotations $\delta\psi$ produced by different isolated linear scales have been obtained for both QSOs and the CMB; nevertheless, calculations have been only performed for the direction $\theta = \pi/4$, $\phi = \pi/2$ and, moreover, the approximating condition $A_{v0} \sim v^{\pm}_{c0R} = v^{\pm}_{c0I}$ has been used; therefore, more general cases must be studied. It is done in this section, where two rather general distributions of linear vector modes with appropriate scales are considered to study the CMB (subsection VI A) and QSOs (subsection VI B). These modes are numerically superimposed using appropriate simulations.

Let us now use Eqs. (38) and (39) to calculate $\delta\psi$. According to Eq. (39), the component F_i of vector $\vec{F}$ is the Fourier transform of the function $k^{-1}[v^{+}_{c0}(\vec{k})\epsilon^{+}_{i}(\vec{\kappa}) - v^{-}_{c0}(\vec{k})\epsilon^{-}_{i}(\vec{\kappa})]$; hence, function $\vec{F}(\vec{r})$ can be simulated by using the three-dimensional (3D) fast Fourier transform (FFT). In order to do that, 512^3 cells are considered inside a big box with a size of 2×10^5 Mpc. In this way, the cell size is $\sim$390 Mpc and, consequently, vector modes with spatial scales between 10^4 Mpc and 5×10^4 Mpc can be well described in the simulation. For these scales, it is assumed that $v^{\pm}_{c0R}$ and $v^{\pm}_{c0I}$ are four statistically independent Gaussian variables, and also that each of these numbers has the same power spectrum. The form of this common spectrum is $P(k) = Ak^{n_v}$, where n_v is the spectral index of the vector modes and A is a normalization constant. We also simulate vectors $\vec{h}_0(\vec{r})$ and $\vec{v}_{c0}(\vec{r})$ taking into account that, according to Eqs. (40) and (41), the ith components of these vectors are the FFT transforms of $v^{\pm}_{c0}(\vec{k})\epsilon^{\pm}_{i}(\vec{\kappa})/k^2$ and $v^{\pm}_{c0}(\vec{k})\epsilon^{\pm}_{i}(\vec{\kappa})$, respectively. Three values of the spectral index, $n_v = -3$, $n_v = 0$, and $n_v = 3$, have been considered. The wave number k varies from 10^4 Mpc to 5×10^4 Mpc in all cases. For each spectrum, constant A can be fixed by the condition that, at a chosen redshift, the maximum $\vec{h}(\vec{r})$ components be close to 0.2 in all the box nodes; e.g., for $n_v = -3$ the resulting normalization is $A \simeq 4.5 \times 10^{-4}$ ($A \simeq 8.3 \times 10^{-14}$) for the redshift $z = 2.6$ ($z = 1100$). In all cases one finds $|v_c(\vec{r})| \lll 1$.

After simulating functions F_i, the observer is placed at an arbitrary point located in the central part of the simulation box, where the Fourier transform is expected to be well calculated. Then, the integral in Eq. (38) is performed for (a) quasars characterized by their redshifts (or equivalently, r_e) and the unit vectors $\vec{n}$ pointing to them, and (b) pixels of a CMB map characterized only by $\vec{n}$. Various sets of directions are studied and the rotation angles $\delta\psi$ are obtained by solving the mentioned integral along each direction.

Figure 2 contains a 2D sketch where the reader can see the main characteristics of both the simulations and the photon trajectories; each small square is covered by 5×5 simulation cells (which have a size of $\sim$390 Mpc). The size of the simulation box is 6 times greater than that of the region represented in the figure. The radius of the circumferences correspond to redshifts of 0.5, 2, 2.6, and 1100. The minimum scale ($L_{\min} = 10^4$ Mpc) is also displayed.

The distances (radius of the circumferences) crossed by photons coming from quasars are similar to our minimum spatial scale ($\sim$ 6000 Mpc for $z = 2.6$); hence, the variations of vector $\vec{h}$ along the photon trajectories are smooth and, consequently, the integrations necessary to calculate $\delta\psi$ can be performed easily. Furthermore, in a central cube with 3×10^4 Mpc per edge (15% of the box size in our simulations), we can place 5^3 observers uniformly distributed and separated by a distance of 6000 Mpc. Then, $\delta\psi$

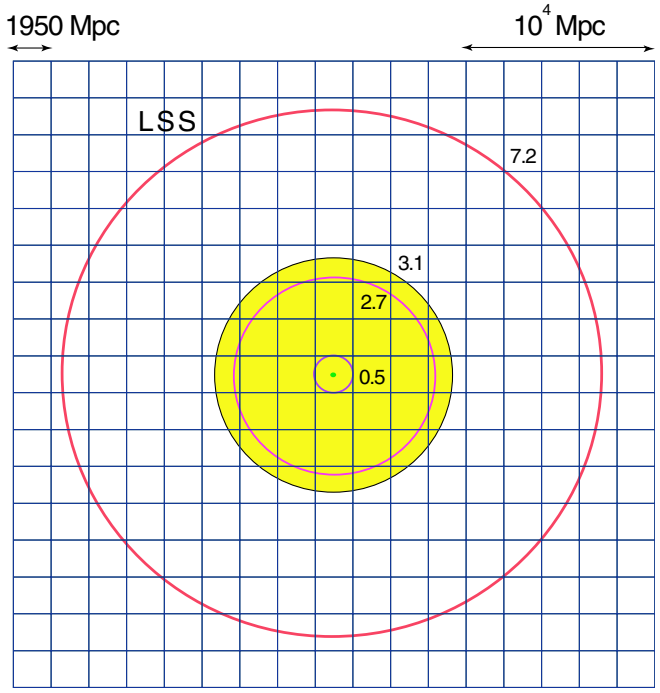

FIG. 2 (color online). 2D sketch showing some characteristics of both the simulations and the emission surfaces. The point at the center of the region represents the observer. Circles whose radius are 0.5, 2.7, 3.1, and 7.2 times the size of the small squares in the panel (1950 Mpc) correspond to the redshifts 0.25, 2, 2.6, and 1100, respectively. LSS stands for last scattering surface (the greatest circle). The shaded (yellow) zone is the region of the QSOs with $z \leq 2.6$. Only $\sim 1/6$ of the simulation box is displayed and each small square is 5 times larger than the simulation cells.

angles can be calculated for each of these observers; thus, from a given simulation, the information we obtain is greater than in the case of one unique observer located, e.g., at the box center.

A. CMB: polarization

In this subsection, CMB photons are moved through the simulation boxes. For $n_v = -3$, the power of the scales close to 5×10^4 Mpc is greater than that of the scales around 10^4 Mpc by a factor of 125; hence, the resulting Skrotskii rotations are essentially produced by vector modes with scales close to 5×10^4 Mpc, which mainly affect the multipoles $\ell = 1$ and $\ell = 2$. Hence, we can be sure that only the first few multipoles of the CMB anisotropy may be affected in this case. For $n_v = 3$, scales close to 10^4 Mpc dominate the Skrotskii effect leading to significant multipoles for $2 < \ell \lesssim 10$ (see first paragraph of Sec. V).

As it is well known, linear polarization of the CMB is produced by Thompson scattering during the recombination-decoupling process. After decoupling, the polarization is only modified during reionization; this is the standard scenario. Hereafter, reionization is forgotten to built up a simple model (reionization effects would be considered in future). Linear polarization at decoupling depends on the kind of FRW perturbations evolving during the recombination-decoupling process; in particular, if vector perturbations are present, they play a relevant role [28]. Functions $F = Q + iU$ and $G = Q - iU$, where Q and U are the usual Stokes parameters [29], are used to describe CMB polarization. Functions F and G can be developed in terms of an appropriate basis of functions and, then, the coefficients E_ℓ and B_ℓ involved in the resulting expansion (see Eqs. (55) in [25]) define the E and B polarization modes. Since the scales of the vector modes we have assumed are very large, the CMB temperature and polarization correlations produced during the recombination-decoupling process are not significantly affected by vector perturbation, excepting the case of multipoles corresponding to small ℓ values, which will be explicitly calculated elsewhere. In the presence of large scale vector modes, the polarization angle ψ varies from decoupling to present time. Hence, parameters Q and U as well as functions F and G and, consequently, the E_ℓ and B_ℓ polarization coefficients undergo transformations.

Let us now look for the amplitude and angular dependence of $\delta\psi$; in order to do that, the redshift is fixed to be that of decoupling, that is to say $z = 1100$. Then, vector modes are superimposed (see above) and $\delta\psi(\vec{n})$ is calculated, where $\vec{n}$ is a unit vector pointing toward the centers of a set of pixels covering the full sky; indeed, a HEALPIx (*hierarchical equal area isolatitude pixelisation of the sphere*, see [30]) pixelisation covering the sky with 3072 pixels is used. Three of the resulting $\delta\psi$ maps are shown in Fig. 3. Top, central, and bottom panels correspond to $n_v = -3$, $n_v = 0$, and $n_v = 3$, respectively. For any spectra, the rms values of the Skrotskii rotations appear to be of a few tenths of degree.

Since the linearity of the vector modes has been appropriately forced, from $z = 0$ to $z = 1100$, to simulate all the maps of Fig. 3, the values of $\delta\psi$ shown in these maps are the largest values produced by linear vector modes. In order to obtain greater values, nonlinear modes (see Sec. V) should be present at redshift $z = 1100$. The angular power spectrum (C_ℓ quantities) of $\delta\psi(\theta, \phi)$ has been calculated for three maps corresponding to $n_v = -3$. This calculation is performed by using the code ANAFAST of the HEALPIx package, which was designed to analyze temperature CMB maps; the four first multipoles are shown in Table I. For $\ell \geq 5$ the resulting multipoles have appeared to be negligible (as it is expected in the case $n_v = -3$, see above). That is compatible with the fact that no small spots (high frequency angular oscillations) there exist in the top panel of Fig. 3. The multipoles corresponding to $n_v = 0$ and $n_v = 3$ are not presented by the sake of briefness, but they are not negligible for a few $\ell \geq 5$ values (see previous discussion). This is consistent with Fig. 3, where we see that there are spots in the central (bottom) panel which are smaller than those of the top (central) one.

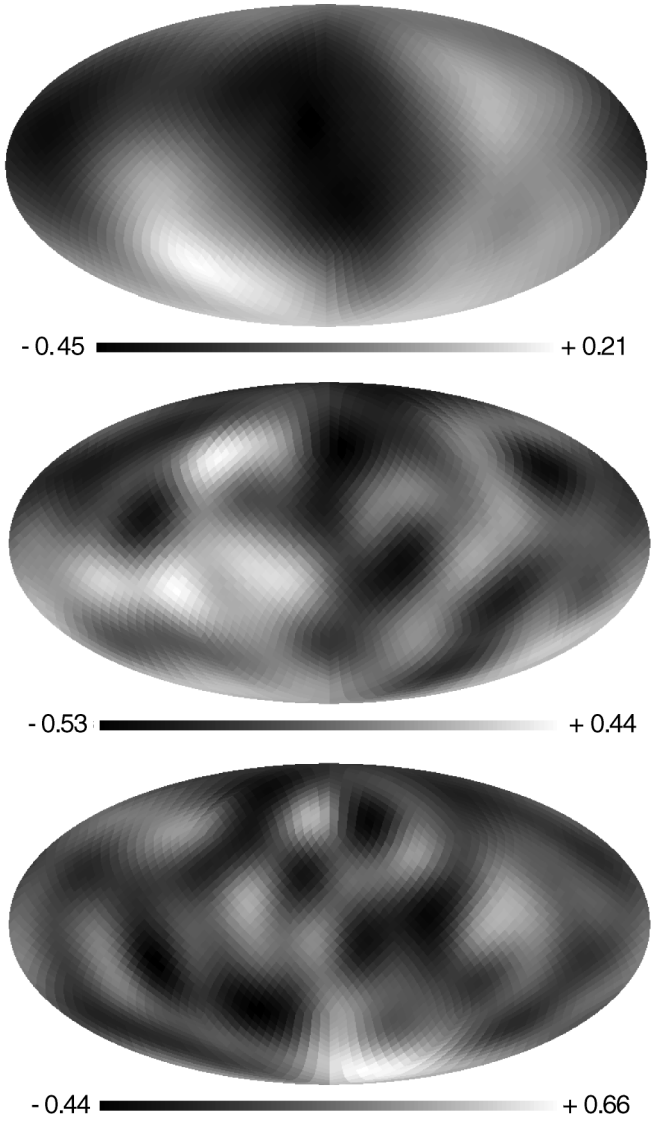

FIG. 3. Each panel shows the Skrotskii rotations (in degrees) of the CMB polarization directions on the full celestial sphere. The statistical realizations of the top, central, and bottom panels correspond to the spectral indexes $n_v = -3$, $n_v = 0$, and $n_v = 3$, respectively.

The magnitude and the orientation of the polarization vector $\vec{P}$ are given by the equations $P^2 = U^2 + Q^2$ and $\tan(2\psi) = U/Q$, respectively. Since P does not change along the null geodesics and condition $\delta\psi \ll 1$ is always satisfied, the variations of U and Q are found to be $\delta U = 2Q\delta\psi$ and $\delta Q = -2U\delta\psi$. Then, one gets the following relations: $\delta F = 2iF\delta\psi$ and $\delta G = -2iG\delta\psi$. Finally, we are interested in the order of magnitude of δE_ℓ and δB_ℓ, where E_ℓ and B_ℓ are the coefficients involved in Eqs. (55) of Ref. [25]. An exact calculation of these quantities is complicated as a result of the angular dependence of $\delta\psi$; nevertheless, taking into account that this dependence is smooth (almost constant values in large sky regions), we can get a good estimate by considering a constant appropriate $\delta\psi$ value, e.g. the rms value corresponding to a standard simulation. Thus, one obtains

$$\delta E_\ell = -2\delta\psi B_\ell, \qquad \delta B_\ell = 2\delta\psi E_\ell. \tag{54}$$

The larger $\delta\psi$, the greater the polarization effects.

For the map of the top panel of Fig. 3, we have found $\delta\psi_{rms} = 0.19°$ and, the second of Eqs. (54) gives then $\delta B_\ell = 6.6 \times 10^{-3} E_\ell$. Taking into account this relation and the fact that the Wilkinson Microwave Anisotropy Probe (WMAP) satellite [31] has detected E-mode polarization with a level of $\sim 0.3\mu K$, one concludes that Skrotskii rotations contribute to the B polarization at a level of $\simeq 0.002\mu K$, which is too small to be detected with the PLANCK satellite in the near future. Furthermore, for a tensor to scalar ratio $r = 0.3$ (upper bound for some simple inflationary models, see [31]), the expected level of the B-mode is $\sim 0.03\mu K$, which could be detected with PLANCK; in this case, the first of Eqs. (54) leads to the conclusion that the level of the Skrotskii contribution to the E mode is $\sim 2 \times 10^{-4}\mu K$, which is very small. Fortunately, new projects are being designed to detect low levels of B polarization for very small ℓ values. For example, the mission SAMPAN (satellite for analyzing microwave polarization anisotropies) has been designed to measure these multipoles for $r > 1.5 \times 10^{-4}$, namely, for a B signal whose level is greater than $\sim 7 \times 10^{-4}\mu K$. This means that future satellites should be able to detect very low signals smaller than the Skrotskii corrections to the B polarization we have estimated (at a level of $\simeq 0.002\mu K$).

TABLE I. Multipoles C_1 to C_4 for three $\delta\psi$ simulations based on a power spectrum with $n_v = -3$.

Realization	C_1	C_2	C_3	C_4
1	0.015	0.023	0.006	0.0007
2	0.052	0.011	0.006	0.0004
3	0.008	0.064	0.005	0.0012

B. QSOs: angular and redshift dependence of $\delta\psi$

The Skrotskii rotation of a quasar depends on the parameters z, θ, and ϕ. In this subsection, angle $\delta\psi$ is calculated for three sets of QSOs characterized by fixed values of two of these parameters. Results are presented in Fig. 4. In the top (central) panel, the fixed parameters are the redshift $z = 2$ and the angle ϕ (θ), which takes on the value $\phi = \pi/5$ ($\theta = \pi/8$). Various simulations have been developed and many observers have been located in the central part of the boxes to calculate $\delta\psi$ for each of the above quasar sets. Three curves obtained for different simulations and observer positions have been selected and displayed in the top and central panels, where it is pointed out the fact that functions $\delta\psi(\theta, \pi/5)$ and $\delta\psi(\pi/8, \phi)$ always are smooth. The same occurs for other fixed values of θ and ϕ different from $\pi/8$ and $\pi/5$, which

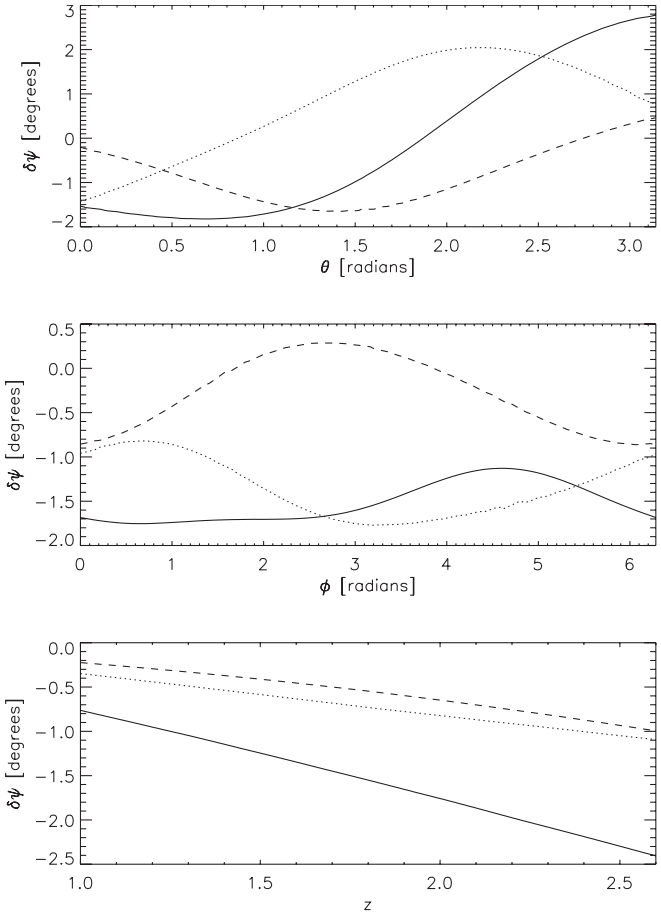

FIG. 4. Dotted, dashed, and solid lines correspond to different simulations of the vector perturbations. The observer has been located in the central part of the simulation box in the three cases. Top, central, and bottom panels exhibit functions $\delta\psi(\theta)$ (for $\phi = \pi/8$ and $z = 2$), $\delta\psi(\phi)$ (for $\theta = \pi/5$ and $z = 2$), and $\delta\psi(z)$ (for $\phi = \pi/8$ and $\theta = \pi/5$), respectively.

means that function $\delta\psi(\theta, \phi)$ has not high frequency variations. This function smoothly varies as θ and ϕ take values on the intervals $[0, \pi]$ and $[0, 2\pi]$, respectively. It is easily understood taken into account Eqs. (38) and (39); in fact, suppose that an observer is at the center of a certain cube covered by 5^3 cells observing QSOs at $z < 0.25$. In such a case, photons come from the smallest circle and they move inside the mentioned cube whose size is $\sim$1950 Mpc (see Fig. 2). Taking into account Eq. (38) and the fact that vector $\vec{F}$ only undergoes small variations inside the cube, one easily concludes that the angular dependence of $\delta\psi$ [fixed by the term $\vec{n} \cdot \vec{F}(\vec{r})$] is of the form $F_1 \sin\theta \cos\phi + F_2 \sin\theta \sin\phi + F_3 \cos\theta$, with almost constant values of F_1, F_2, and F_3. Hence, the multipolar expansion of $\delta\psi$ only involves dipolar and quadrupolar components but no higher multipoles (there are no high frequency angular oscillations). If our observer is analyzing the light arriving from QSOs placed at redshift $z = 2.6$, photons move inside the shaded (yellow) zone, whose size is $\sim$12000 Mpc (similar to the minimum scale in our simulations); thus, the vector field $\vec{F}(\vec{r})$ is not constant inside this zone, but it varies smoothly and, consequently, this vector and the $\delta\psi$ angles take on similar values for close directions. By this reason, no high frequency angular variations of $\delta\psi(\theta, \phi)$ can appear.

In the bottom panel of Fig. 4, the absolute value of the angle $\delta\psi$ appears to be an increasing function of z for the fixed angles $\phi = \pi/8$ and $\theta = \pi/5$. The same occurs for any pair of angles (θ, ϕ).

VII. DISCUSSION AND PROSPECTS

Vector perturbations of a FRW universe are generated in some cosmological scenarios involving brane worlds [2], topological defects [3], and vector fields (see Sec. IV B). Therefore, the study of the physical effects produced by these modes deserve attention. Only if these effects are estimated, the existence of vector perturbations may be discussed. Large enough effects could be detected, whereas other effects might be used to put bounds to the amplitudes and scales of vector modes in nature, restricting thus the scenarios where they appear. In this paper, a systematic study of the effects produced by vector modes is started.

A flat ΛCDM universe (concordance model) containing vector cosmological modes with very large spatial scales is assumed. In this universe, a Skrotskii effect—similar to that produced by the space-time of a rotating body—is calculated for rather general distributions of vector modes which evolve in the linear regime under the condition $\Pi^{\pm} = 0$. In this scenario, the polarization angle of the radiation emitted by any source undergoes a certain Skrotskii rotation. Quasars and points of the last scattering surface have been considered as sources. The initial correlations among the polarization angles changes because the Skrotskii rotations are different for distinct sources. Observations must be designed to measure these correlation changes, but measurements will be only possible for large enough $\delta\psi$ rotations.

In previous sections we have presented: (i) analytical calculations leading to explicit formulas for the Skrotskii effect of vector modes, and (ii) the design of appropriate numerical simulations allowing the estimation of this effect. Our main conclusion is that the contribution of linear vector perturbations to the B-mode of the CMB polarization (for small ℓ values) might be larger than that produced by cosmological gravitational waves. Data from future satellites should lead either to a detection or to bounds on the vector perturbations amplitudes and scales.

The Skrotskii rotations have been estimated for both quasar distributions and CMB maps. In both cases, calculations are based on simulations. Three spectra have been considered to get Gaussian distributions of vector modes. All these spectra have been normalized using the same condition (see Sec. VI). Condition $\Pi^{\pm} = 0$ has been assumed. It implies that vector modes decay during the

matter dominated era. Using these decaying modes (the worst situation to get large $\delta\psi$ angles), two independent cases have been considered: (1) vector modes are linear in the redshift interval (0,2.6) and nonlinear for $z > 2.6$ (QSOs study), and (2) vector modes are linear in the interval (0,1100) and nonlinear for $z > 1100$ (CMB analysis); thus, the maximum rotations produced by linear modes, for QSOs with $z < 2.6$, are obtained in case 1, whereas the maximum Skrotskii effect for linear modes and CMB maps appears in case 2.

For QSOs with $z < 2.6$ (case 2), the Skrotskii rotations have reached values of a few degrees, which are too small to explain the correlations and alignments strongly suggested by the statistical analysis ([32,33]) of recent QSO observations [19]. Only a small part of the effect could be due to linear vector modes. Values of $\delta\psi$ one order of magnitude greater than those obtained from linear freely decaying ($\Pi^{\pm} = 0$) vector modes would be necessary to obtain correlations comparable to those suggested by recent observations. These large rotations could be obtained in various models, among them, let us list those based on the existence of: (a) large scale nonlinear vector modes with $\Pi^{\pm} = 0$ (see Sec. V), (b) anisotropic stresses, $\Pi^{\pm} \neq 0$, produced by some unknown field, which could prevent the free decaying of the involved modes (see Sec. IV B), (c) branes in a 5D [2], and (d) topological defects [3]. More work is necessary to analyze possibilities (a)–(d) in detail. That is one of our main prospects.

For the CMB (case 1), the rms values of $\delta\psi$ appear to be of a few tenths of a degree. Future experiments designed to measure B_ℓ quantities (for small ℓ) could detect signals smaller than the B polarization induced by the vector modes we have considered. For small enough values of r, the vector induced B signal could be either comparable or greater than that produced by primordial gravitational waves. This fact should be taken into account to interpret observations of future satellites. Neither the amplitude of the gravitational waves nor that of the vector modes are known, which means that the effects produced by different amplitudes of both FRW perturbations must be predicted for comparisons.

ACKNOWLEDGMENTS

This work has been supported by the Spanish Ministerio de Educación y Ciencia, MEC-FEDER projects No. AYA2003-08739-C02-02 and No. FIS2006-06062.

[1] J. M. Bardeen, Phys. Rev. D **22**, 1882 (1980).
[2] R. Maartens, Phys. Rev. D **62**, 084023 (2000).
[3] E. F. Bunn, Phys. Rev. D **65**, 043003 (2002).
[4] G. V. Skrotskii, Dokl. Akad. Nauk SSSR **114**, 73 (1957) [Sov. Phys. Dokl. **2**, 226 (1957)].
[5] B. Mashhoon, Phys. Rev. D **11**, 2679 (1975).
[6] F. Fayos and J. Llosa, Gen. Relativ. Gravit. **14**, 865 (1982).
[7] H. Ishihara, M. Takahashi, and A. Tomimatsu, Phys. Rev. D **38**, 472 (1988).
[8] S. Bildhauer, Astron. Astrophys. **219**, 25 (1989).
[9] N. Yu. Gnedin and I. G. Dymnikova, Zh. Eksp. Teor. Fiz. **94**, 26 (1988) [Sov. Phys. JETP **67**, 13 (1988)].
[10] M. Nouri-Zonoz, Phys. Rev. D **60**, 024013 (1999).
[11] I. Yu. Kobzarev and K. G. Selivanov, Zh. Eksp. Teor. Fiz. **94**, 1 (1988) [Sov. Phys. JETP **67**, 1955 (1988)].
[12] S. Kopeikin and B. Mashhoon, Phys. Rev. D **65**, 064025 (2002).
[13] M. Sereno, Phys. Rev. D **69**, 087501 (2004).
[14] V. A. Korotkii and Yu. N. Obukhov, Zh. Eksp. Teor. Fiz. **99**, 22 (1991) [Sov. Phys. JETP **72**, 11 (1991)]; V. A. Korotkii and Yu. N. Obukhov, Zh. Eksp. Teor. Fiz. **108**, 1889 (1995) [Sov. Phys. JETP **81**, 1031 (1995)].
[15] V. F. Panov and Yu. G. Sbytov, Zh. Eksp. Teor. Fiz. **101**, 769 (1992) [Sov. Phys. JETP **74**, 411 (1992)]; V. F. Panov and Yu. G. Sbytov, Zh. Eksp. Teor. Fiz. **114**, 769 (1998) [JETP **87**, 417 (1998)].
[16] R. A. Matzner and B. W. Tolman, Phys. Rev. D **26**, 2951 (1982).
[17] J. A. Morales and E. Navarro, in *Proceeding of the Spanish Relativistic Meeting, ERE-2001*, edited by L. Fernández Jambrina and L. M. González-Romero (Springer-Verlag, Berlin, Heidelberg, 2003), pp. 306–314.
[18] P. Birch, Nature (London) **298**, 451 (1982).
[19] D. Hutsemékers, R. Cabanac, H. Lamy, and D. Sluse, Astron. Astrophys. **441**, 915 (2005).
[20] V. B. Bezerra, H. J. Mosquera Cuesta, and C. N. Ferreira, Phys. Rev. D **67**, 084011 (2003).
[21] C. Wolf, Apeiron **8**, 87 (2001).
[22] D. G. Kendall, Q. Jl R. Atsron. Soc. **25**, 147 (1984).
[23] T. R. Jaffe, A. J. Banday, H. K. Eriksen, K. M. Górski, and F. K. Hansen, Astrophys. J. **629**, L1 (2005).
[24] D. N. Spergel *et al.*, astro-ph/0603449.
[25] W. Hu and M. White, Phys. Rev. D **56**, 596 (1997).
[26] E. W. Kolb and M. S. Turner, *The Early Universe* (Addison-Wesley, Reading, MA, 1994).
[27] G. Hinshaw *et al.*, astro-ph/0603451.
[28] W. Hu and M. White, New Astron. Rev. **2**, 323 (1997).
[29] M. Born and E. Wolf, *Principles of Optics* (Cambridge Univerisity Press, Cambridge, England, 1999).
[30] K. M. Górski, E. Hivon, and B. D. Wandelt, in *Proceedings of the MPA/ESO Conference on Evolution of Large Scale Structure*, edited by A. J. Banday, R. K. Sheth, and L. Da Costa (Printpartners Ipskamp, Enschede, 1999), pp. 37–42 [astro-ph/9812350].
[31] L. Page *et al.*, astro-ph/0603450.
[32] D. Hutsemékers, Astron. Astrophys. **332**, 410 (1998).
[33] P. Jain, G. Narain, and S Sarala, Mon. Not. R. Astron. Soc. **347**, 394 (2004).